Supplementary Information

Mitochondria-Targeting Ceria Nanoparticles as Antioxidants for Alzheimer's Disease

Hyek Jin Kwon, [†,‡,⊥] *Moon-Yong Cha,* [§,⊥] *Dokyoon Kim,* [†] *Dong Kyu Kim,* [§] *Min Soh,* [†,‡] *Kwangsoo Shin,* [†,‡] *Taeghwan Hyeon,* [*,†,‡] *Inhee Mook-Jung* [*,§]

[†]Center for Nanoparticle Research, Institute for Basic Science (IBS), Seoul 151-742, Republic of Korea, [‡]School of Chemical and Biological Engineering and Institute of Chemical Processes, Seoul National University, Seoul 151-742, Republic of Korea, [§]Department of Biochemistry and Biomedical Sciences, Seoul National University College of Medicine, Seoul 110-799, Republic of Korea.

[⊥]These authors contributed equally to this work.

* Address correspondence to

thyeon@snu.ac.kr,

inhee@snu.ac.kr.

Methods and Experimental

1. Materials.

The following reagents were purchased from Sigma-Aldrich Inc. (St. Louis, MO, USA): (3-carboxypropyl)triphenyl-phosphonium bromide, (3-CTPP), N-(3-dimethylaminopropyl)-N′-ethylcarbodiimide hydrochloride (EDC), N-hydroxysuccinimide (NHS), and triethylamine (TEA), cerium acetate (98%), xylene (98.5%), hydrogen peroxide (H2O2, 30%), and fluorescein isothiocyanate (FITC). Oleylamine (approximate C18-content of 80-90%) was purchased from Acros Organics (Geel, Belgium). Hexane (99%), ethanol (99%), chloroform (99%), acetone (99%) and plasma from human were purchased from Samchun Chemicals (Seoul, Korea). The SOD assay and Amplex® red hydrogen peroxide/peroxidase assay kits were purchased from Dojindo Laboratories (Kumamoto, Japan) and Molecular Probes, Inc. (Eugene, OR, USA), respectively. The 1,2-distearoyl-sn-glycero-3-phosphoethanolamine-N-[methoxy(polyethylene glycol)-2000] (mPEG-2000-PE) and 1,2-distearoyl-sn-glycero-3-phosphoethanolamine-N-[amino(polyethylene glycol)-2000] (DSPE-PEG(2000)-amine) were purchased from Avanti Polar Lipids, Inc. (Alabaster, AL, USA).

2. Ceria nanoparticle synthesis.

Ceria nanoparticles were formed by hydrolytic sol-gel reactions. Briefly, 0.43 g cerium(III) acetate (1 mmol) and 3.25 g oleylamine (12 mmol) were dissolved in 15 mL xylene. The mixture solution was stirred vigorously for 12 h at room temperature and then heated to 90 °C with a heating rate of 2 °C/min under a vacuum. Deionized water (1 mL) was rapidly injected into the heated solution to initiate the sol-gel reaction, as indicated by a color change from purple to cloudy yellow. The reaction solution was then incubated at 90 °C for 3 h until transparent prior to cooling to room temperature. Ceria nanoparticles were precipitated by adding 100 mL acetone, harvested by centrifugation, and then resuspended in chloroform to a final concentration of 10 mg/mL.

3. Synthesis of DSPE-PEG-TPP and FITC-conjugated DSPE-PEG.

8.6 mg 3-CTPP (20 μmol), 11.5 mg EDCI (60 μmol), 6.9 mg NHS (60 μmol), and 20 μL triethylamine were dissolved in 1 mL chloroform. The solution was stirred vigorously for 2 h at room temperature. Then, it was added to a second solution of 50 mg DSPE-PEG-amine dissolved in 2 mL chloroform. The mixture solution was stirred for 24 h at room temperature. To produce FITC-conjugated DSPE-PEG, 7.8 mg FITC (20 μmol), 20 μL triethylamine, and 50 mg DSPE-PEG-amine were dissolved in 10 mL chloroform, and the solution stirred vigorously for 24 h at room temperature.

4. Synthesis of water-dispersive TPP-ceria NP.

DSPE-PEG-TPP (25 mg) and ceria NPs (8 mg) were mixed in 25 mL chloroform. The solution was evaporated using a rotary evaporator and vacuumed at 80 °C for 1 h. 8 mL of deionized water was then added into the flask and sonication was performed. The transparent, light-yellow suspension was filtered by syringe filter of 0.2 μm pore size. To remove the free DSPE-PEG-TPP, we purified the TPP-ceria NPs thoroughly by treating the obtained NPs sequentially using high-speed ultracentrifugation at 450,000 x g for 2 hours, filtration using an Amicon® centrifugal filter with a cut-off molecular weight of 50 kDa, and dialysis using a Slide-A-Lyzer dialysis cassette with a 10 kDa molecular weight cut-off (Thermo, Rockford, IL, USA) for 24 hours.

5. Synthesis of water-dispersive FITC-conjugated TPP-ceria NPs and FITC-conjugated ceria NPs.
Water-dispersive FITC-conjugated TPP-ceria and FITC-conjugated ceria NPs were obtained by the same procedures for the preparation of water-dispersive TPP-ceria and ceria NPs except that a mixture of FITC-conjugated DSPE-PEG and DSPE-PEG was used (1:50 ratio of DSPE-PEG-FITC to total DSPE-PEG-TPP).

6. Synthesis of water-dispersive TPP-iron oxide NPs, iron oxide NPs, FITC-conjugated TPP-iron oxide NPs.
water-dispersive TPP-iron oxide NPs, iron oxide NPs, FITC-conjugated TPP-iron oxide NPs and iron oxide NPs were obtained by the same procedures for the preparation of water-dispersive TPP-ceria and ceria NPs. Iron oxide NPs with 3 nm, 10 nm, and 18 nm size were synthesized according to previous publication.

7. Transmission electron microscopy (TEM).
Ceria and TPP-ceria NP samples were prepared by adding the solutions dropwise onto carbon-coated copper grid, and leaving them to evaporate. Transmission electron microscope (TEM) analysis was then performed using a JEOL JEM-2010 TEM (JEOL, Tokyo, Japan) operating at 200 kV.

8. Nuclear Magnetic Resonance (NMR).
DSPE-PEG(2000)-TPP was dissolved in deuterated chloroform and analyzed by ^{1}H NMR using a Varian 500 MHz spectroscope (Varian, Inc., Palo Alto, CA, USA).

9. Measurement of Hydrodiameters and zeta potentials of TPP-ceria or ceria nanoparticle.
Hydrodiameters and zeta potentials for the TPP-ceria NPs and ceria NPs were measured by dynamic light scattering (DLS) with a Zetasizer Nano-ZS system (Malvern Instruments, Inc., Worcestershire, UK) and disposable folded capillary cells..

10. Inductively coupled plasma mass spectrometry (ICP-MS) analysis.
Elemental analysis was performed using an inductively coupled plasma atomic emission spectrometer (ICP-AES, ICPS-1000IV, Shimadzu, Japan) and an inductively coupled plasma mass spectrometer (ICP-MS, ELAN 6100, Perkin-Elmer).

11. SOD activity assay and catalase activity assay.
The superoxide scavenging activity was assessed using a SOD assay kit (Sigma-Aldrich). First, increasing concentrations of ceria and TPP-ceria NPs were diluted in 200 μL WST-1 (water-soluble tetrazolium salt; (2-(4-iodophenyl)-3-(4-nitrophenyl)-5-(2,4-disulfo-phenyl)-2H-tetrazolium, monosodium salt) solution with cerium concentrations of 0, 0.093, 0.187, 0.375, 0.75, and 1.5 mM and added to each well in triplicate. SOD coupling reactions were initiated by the addition of 20 μL xanthine oxidase solution, and then incubated at 37 °C for 20 min. Absorbance at 450 nm, which is proportional to SOD activity, was read using a microplate reader (Victor X4, Perkin-Elmer, Waltham, MA, USA). 50 U/mL SOD was defined as the activity of the enzyme that inhibits the reduction reaction of WST-1 with superoxide anion by 50% in experiments quantifying SOD-mimetic activity. 3 repeated sets of measurements was performed. The catalase activity of ceria and TPP-ceria NPs was measured by an Amplex® Red Hydrogen Peroxide/Peroxidase assay kit (Molecular Probes Inc.). In the presence of catalase activity, Amplex Red reagent (10-acetyl-3,7-

dihydroxyphenoxazine) reacts with hydrogen peroxide to yield a red fluorescent resorufin oxidation product. For this, ceria or TPP-ceria NPs were diluted in 1X reaction buffer containing 100 μM Amplex® Red reagent, 2 mM hydrogen peroxide, with different cerium concentrations of 0, 0.25, 0.5, and 1 mM. Then, 50 μL of the above solution was added to microplate wells in triplicate. The microplate was protected from light and incubated at room temperature for 30 min. The absorbance at 490 nm was then measured with a microplate reader. 1mU/ml HRP worked as the 100% control when measuring the catalase-mimetic activity. 3 repeated sets of measurements was performed.

12. Cell culture.
HeLa, HT22, U373 and SH-SY5Y cells were cultured in minimum essential medium (MEM) or MEM/F12 media supplemented with 10% heat-inactivated fetal bovine serum, respectively. Cell were maintained at 1×10^5 cells/mL at 37 °C in a humidified atmosphere of 5% CO_2.

13. Cell viability assays.
SH-SY5Y and HT22 were seeded at 10,000 cells per well and cultured for 24 h. Ceria or TPP-ceria NPs were diluted in cell media and added to triplicate microplate wells containing increasing cerium concentrations (0, 0.015, 0.25, 0.5, and 1 mM), and then 20 μL of 5 mg/mL 3-[4,5-dimethylthialzol-2-yl]-2,5-diphenyltetrazolium bromide (MTT) was added to each well. The microplate was incubate at 37 °C for 4 h, and then the media was replaced with 200 μL DMSO per well. Cell viability was determined by measuring absorbance at 595 nm.

14. Mitochondrial ROS scavenging activity analysis.
SH-SY5Y, HT22, and U373 cells were seeded at 1×10^5 per well in a 24-well plate and cultured for 24 h. Ceria or TPP-ceria NPs were diluted in cell media with 0.1 mM of cerium concentrations and added to wells containing 5 μM Aβ. The plate was incubated at 37 °C for 12 h, at which point the medium was removed and cells were incubated with 1 mL 5 μM MitoSOX® cell media at 37 °C for 10 min. Then, the cells were washed three times with DPBS, harvested by trypsinization, and fixed in 3% formaldehyde for 10 min. Fixed cells were collected by centrifugation and resuspended in 0.5 mL PBS for flow cytometry analysis on an Accuri™ C6 flow cytometer (BD Biosciences, Franklin Lakes, NJ, USA) with a 473 nm laser and 575 nm filter. Relative mitochondrial ROS scavenging activity was determined by the fluorescence intensity of MitoSOX®.

15. Nanoparticle subcellular localization.
HeLa and SH-SY5Y cells (1×10^5) were seeded in 2 mL media in a confocal dish and incubated for 24 h. The media were then replaced with 2 mL media containing 0.5 μM MitoTracker® Orange CMTMRos (Invitrogen-Life Technologies, Carlsbad, CA) and 0.5 μM LysoTracker® Blue DND-22(Invitrogen-Life Technologies, Carlsbad, CA) for 30 min at 37 °C. Cells were washed three times with DPBS and then cultured in cell media containing FITC-conjugated ceria or TPP-ceria NPs and 1 mM cerium at 37 °C for 12 h. NP movement and subcellular localization were monitored by confocal microscopy with an LSM-780 microscope (Carl Zeiss, Oberkochen, Germany). Colocalization coefficients were obtained by analyzing the microscopic images with ZEN2012 software (Carl Zeiss, Oberkochen, Germany).

16. Animal experiments.

The 5XFAD transgenic mouse model develops severe amyloidal plaques and exhibits an AD-like phenotype. For our analyses, 5XFAD mice overexpressing the human amyloid precursor protein 695 isoform (APP695) harboring three familial AD (FAD) mutations (Swedish: KM670/671NL; Florida: I176V, and London: V717I) and human presenilin 1 (PSEN1) containing the M146L and L286V mutations under the transcriptional control of the mouse *Thy1* promoter were purchased from Jackson Laboratories (Bar Harbor, ME, USA). Six-month-old 5XFAD and B6/SJL littermate control mice were used for tissue analysis.

17. Stereotaxic injections.

The 4-month-old mice from the WT + saline, transgenic (Tg) + saline, Tg + FITC-conjugated ceria NPs, and Tg + FITC-conjugated TPP-ceria NPs treatment groups were anesthetized with isofluorane and placed in a stereotaxic frame (myNeuroLab, St. Louis, MO, USA). Unilateral subicular injections of vehicle, ceria NPs, or TPP-ceria NPs (-4.16 mm AP, 3.25 mm ML, and -4.0 mm DV) were performed using a stereotaxic apparatus as described by the Paxinos and Watson atlas. Mice were injected with saline, ceria NPs, or TPP-ceria NPs using a Hamilton microsyringe (3 μL, 0.5 μL/min, 26-gauge syringe). To examine the therapeutic effects of ceria or TPP-ceria, immunofluorescence and biochemical analyses were performed 2-months after surgery. Animal treatment and maintenance were approved by the Ethics Review Committee for Animal Experimentation in Seoul National University.

18. Immunostaining.

Mice were anesthetized with a mixture of Zoletil (Virbac, Carros, France) and Rompun (Bayer Korea, Seoul, Korea) and perfused with 4% paraformaldehyde solution in phosphate-buffered saline (PBS). Brains were subsequently fixed in 0.1 M phosphate buffer containing 4% paraformaldehyde for 20 h at 4 °C and incubated in a 30% sucrose solution in 0.05 M PBS for 72 h prior to sectioning into 30-μm slices using a freezing cryostat (Leica, Wetzlar, Germany). For immunolabeling, tissue sections were incubated at 4 °C overnight with anti-NeuN antibody (1:1,000; Millipore, Billerica, MA, USA), anti-GFAP antibody (1:1,000; Invitrogen, Carlsbad, CA, USA) and anti-Iba1 antibody (1:500; Wako, Tokyo, Japan). For Aβ immunofluorescence, tissue sections were pretreated with 70% formic acid for 20 min prior to incubation with anti-biotin-labeled 4G8 antibody (1:2000; Covance, Princeton, NJ, USA). Stained tissue sections were then incubated with Alexa 594-conjugated streptavidin, donkey anti-mouse Alexa 594, goat anti-rat Alexa 594, and goat anti-rabbit Alexa 647 (all 1:500; Molecular Probes) for 1 h at room temperature and counterstained with 4'-6-diamidino-2-phenylindole (DAPI, 1:5,000; Sigma-Aldrich) for 10 min prior to imaging.

19. Quantification of immunoreactivity.

For quantification of immunoreactivity, three sections (100-nm apart) from each mouse brain were taken from similar regions. . Five random acquisition areas were considered for each brain section. Stained NeuN-positive cells were counted using Image-Pro Plus (Media Cybernetics, Betheda, MD, USA). To quantify Biotin-4G8, GFAP and Iba-1 positive area, immunofluorescence region in the subiculum areas was analyzed using the Image J software (National Institute of Health, USA).

20. Quantification of cerium ion concentration after administration of TPP-Ceria NPs in brain tissue.

Determination of cerium content in contralateral and ipsilateral side of brain was performed by ICP-MS analysis (ELAN 6100, Perkin-Elmer SCIEX). Brain tissue was dissolved in aqua regia. The resulting solutions were diluted in HNO_3 (2%, 2 ppb, 1:300 v/v). Elemental

analysis was performed using inductively coupled plasma mass spectrometer (ICP-MS, ELAN 6100, Perkin-Elmer)

21. Western blotting analysis.
Brain subiculum tissues were lysed in RIPA buffer (50 mM Tris-HCl pH 7.5, 150 mM sodium chloride, 0.5% sodium deoxycholate, 0.1% SDS, 1% Triton X-100, 2 mM EDTA) containing protease inhibitor cocktail (Sigma-Aldrich). Whole tissue lysates were boiled for 5 min, separated on 4-12% Bis-Tris Nu-PAGE gels (Invitrogen), and then transferred to membranes. Membranes were incubated with anti-4-HNE (Abcam, Cambridge, MA, USA), anti-6E10 (Covance), and anti-GAPDH (Millipore), and enhanced chemiluminescence (ECL; GE Healthcare, Buckinghamshire, UK) was used for signal visualization. Images were captured using a bioimaging analyzer (LAS-3000, Fuji, Tokyo, Japan) and analyzed using Multi-Gauge software (Fuji, Japan).

22. Transmission Electron microscopy for brain tissues.
Brain tissues from 5XFAD mice were sequentially fixed overnight in a mixture of cold 2.5% glutaraldehyde in 0.1 M phosphate buffer (pH 7.2) and 2% paraformaldehyde in 0.1 M phosphate or cacodylate buffer (pH 7.2) before embedding in epoxy resin. The embedded samples were loaded into capsules and polymerized at 38 °C for 12 h and then 60 °C for 48 h. Thin sections were made using an ultramicrotome (RMC MT-XL; RMC Products, Portsmouth, NJ, USA) and collected on a copper grid. Appropriate areas for thin sectioning were cut to 65-nm thickness and stained with saturated 4% uranyl acetate/4% lead citrate prior to TEM before examination with a transmission electron microscope (JEM-1400, JEOL) at 80 kV.

23. Statistical analysis.
Quantitative data were analyzed statistically with Student's t tests or ANOVA by Prism 6 (GraphPad, San Diego, CA, USA).

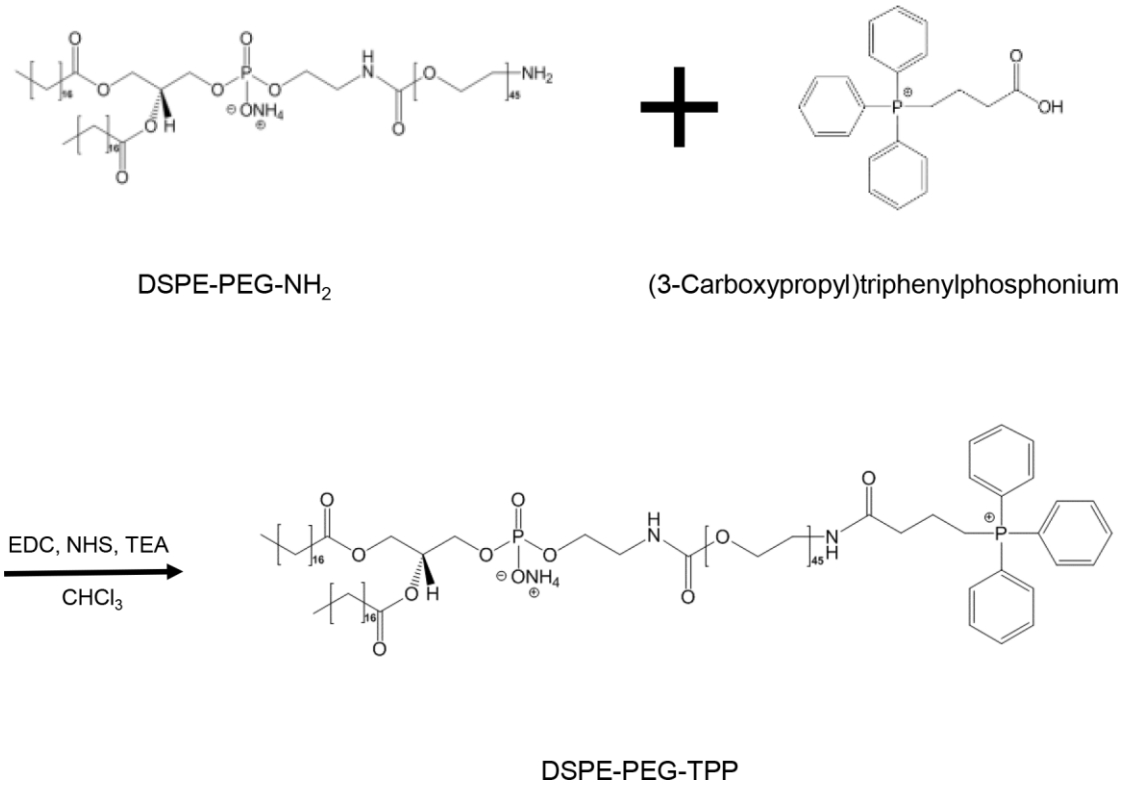

Figure S1. Scheme of DSPE-PEG-NH_2-TPP conjugation. Triphenylphosphonium (TPP) was chemically conjugated to DSPE-PEG-NH_2 by EDC coupling.

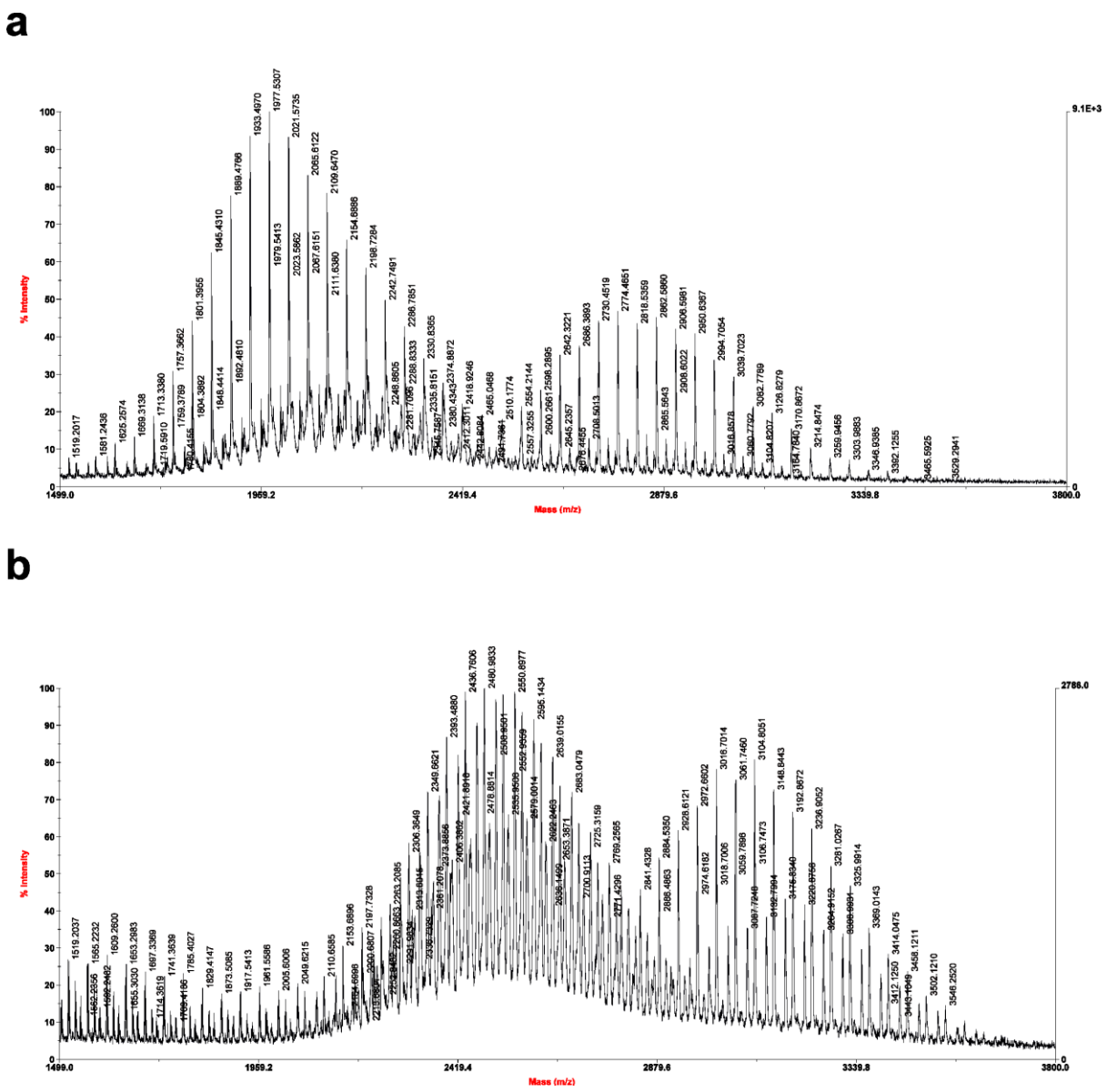

Figure S2. MALDI-TOF spectra of DSPE-PEG-TPP. The molecular weight of DSPE-PEG-NH_2 increased following conjugation with TPP. Molecular weight of TPP is 349.39 g/mol. The increased molecular weight of main peak is approximately 350 g/mol.

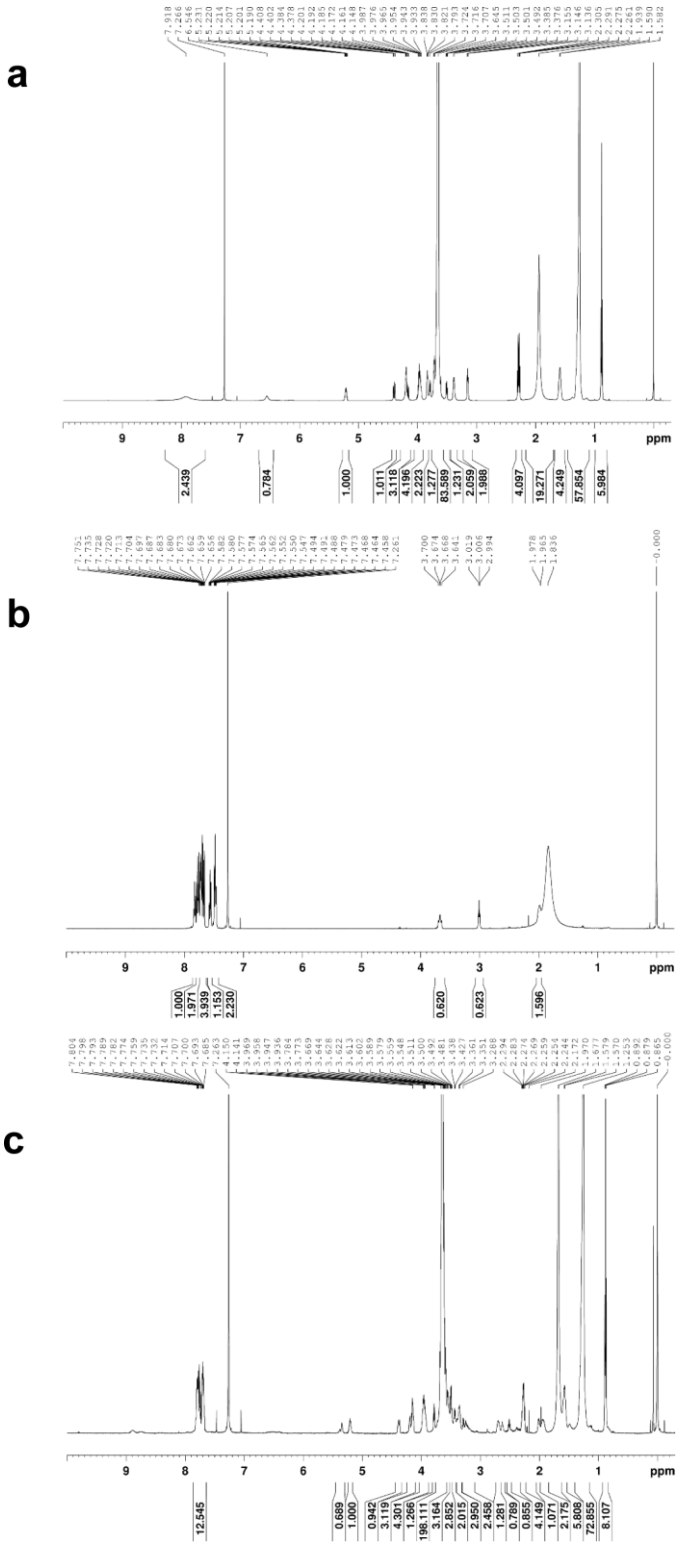

Figure S3. NMR spectra of DSPE-PEG-NH_2, TPP and DSPE-PEG-TPP. **A)** DSPE-PEG-NH_2, **B)** TPP, **C)** DSPE-PEG-TPP.

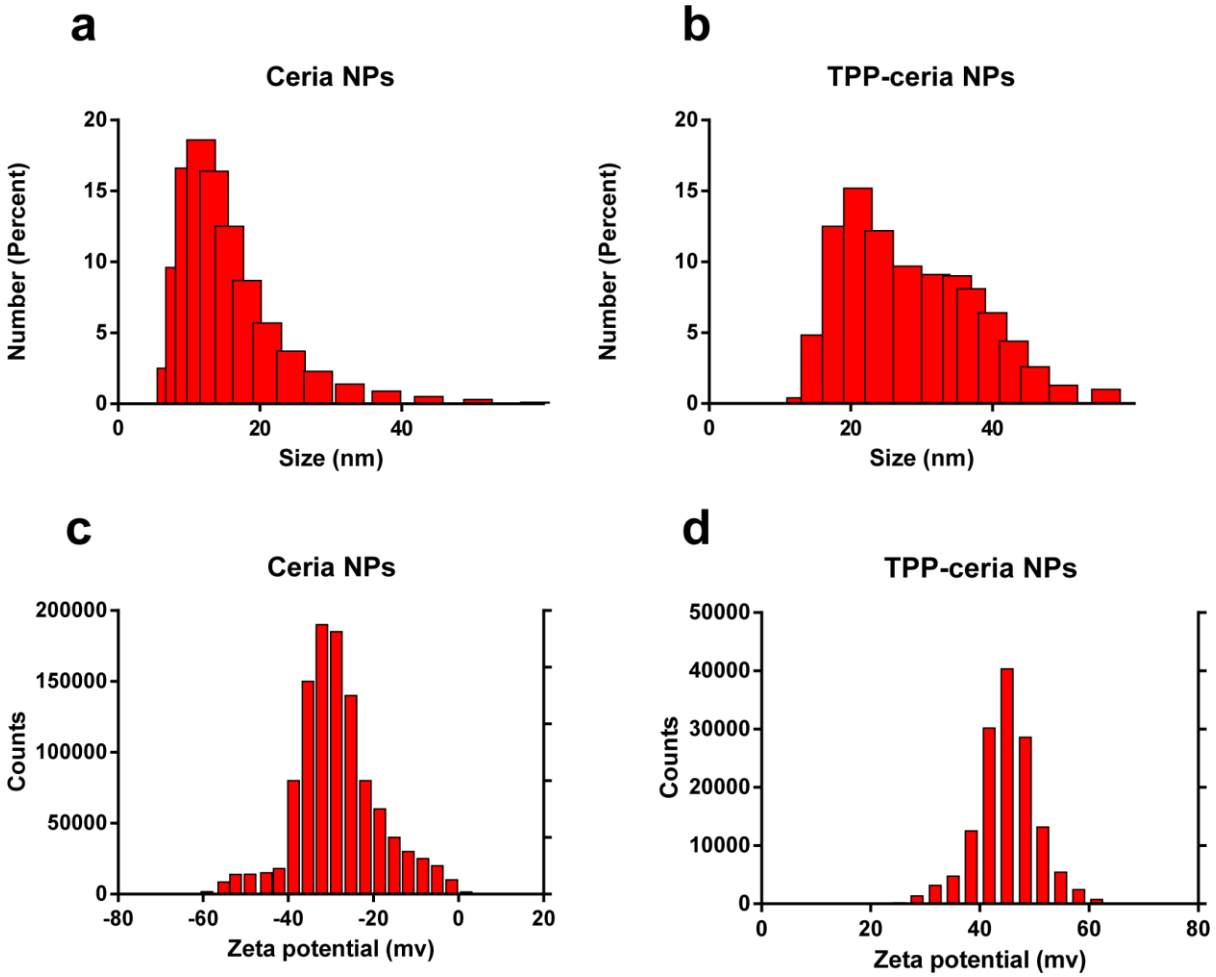

Figure S4. DLS spectra of ceria NPs and TPP-ceria NPs. A) Hydrodynamic diameters of ceria NPs, B) Hydrodynamic diameters of TPP-ceria NPs, C) Zeta potential of ceria NPs, D) Zeta potential TPP-ceria NPs.

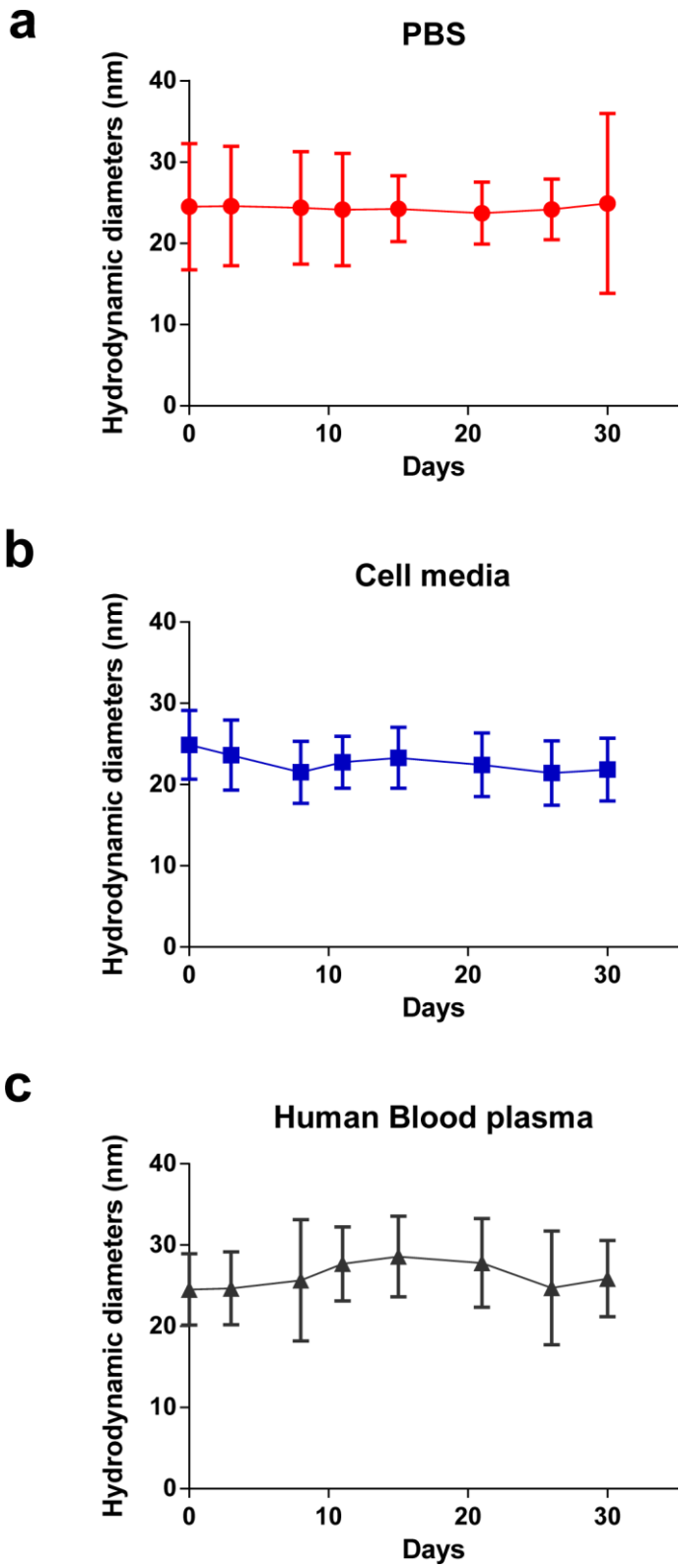

Figure S5. Hydrodynamic diameters of TPP-ceria NPs in A) PBS, B) Cell media (DMEM+10% FBS), C) Human blood plasma.

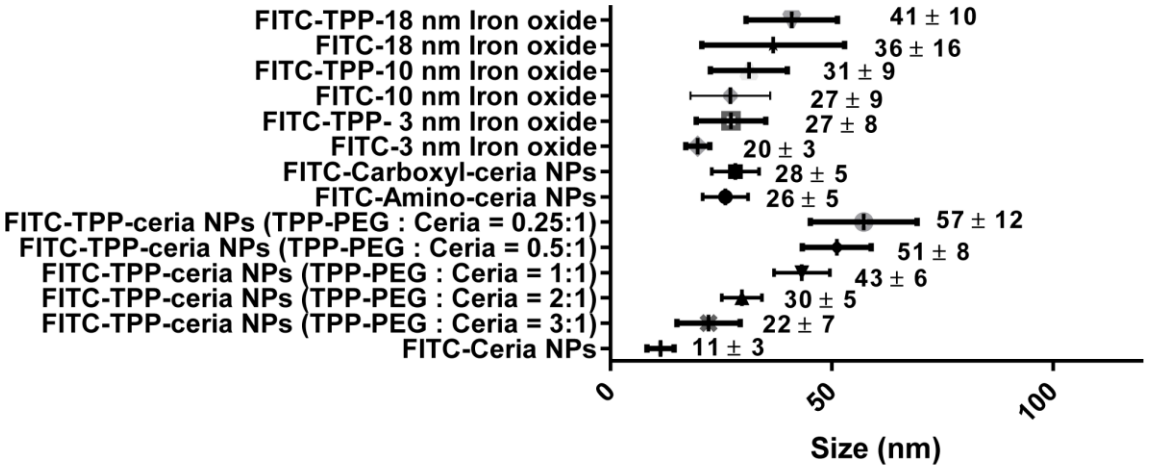

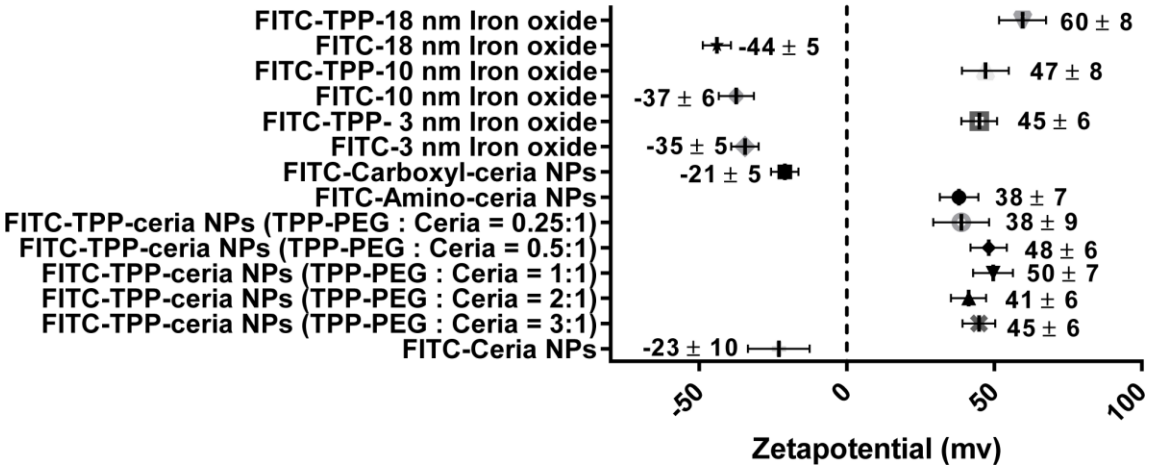

Figure S6. Hydrodynamic diameters and zeta potentials of FITC conjugated TPP-ceria NPs, iron oxide NPs, carboxyl-ceria NPs, amino-ceria NPs and ceria NPs. a) Hydrodynamic diameters of FITC conjugated TPP-ceria NPs, iron oxide NPs, carboxyl-ceria NPs, amino-ceria NPs and ceria NPs. b) zeta potentials of FITC conjugated TPP-ceria NPs, iron oxide NPs, carboxyl-ceria NPs, amino-ceria NPs and ceria NPs.

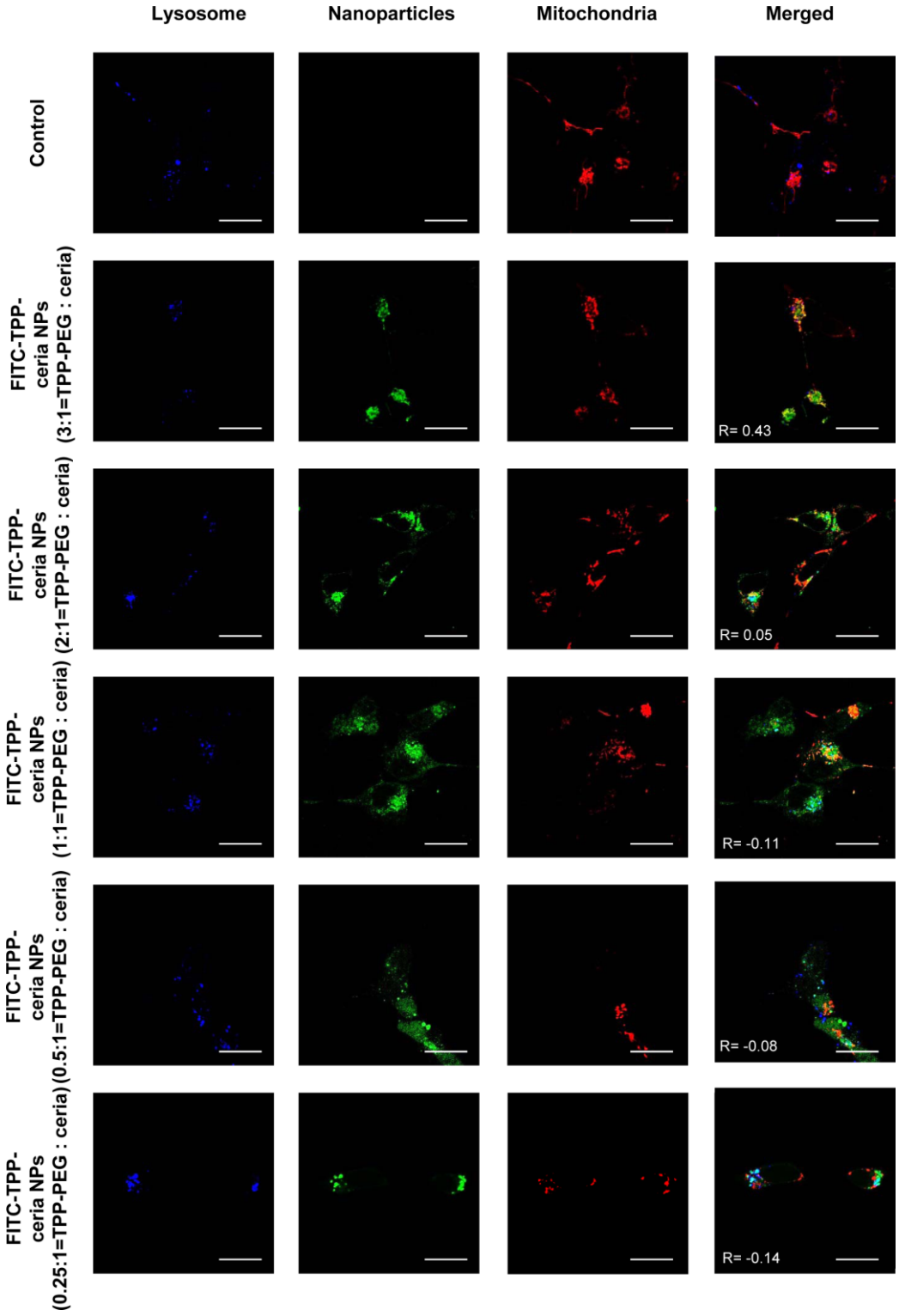

Figure S7. Representative confocal fluorescence microscopy images showing the subcellular colocalization of FITC-conjugated TPP-ceria with different mass ratio of TPP-DSPE-PEG to ceria NPs (green) in SH-SY5Y. SH-SY5Y cells were stained with LysoTracker (blue) and MitoTracker (red). Colocalization of FITC-conjugated TPP-ceria NPs and mitochondria (red) is shown in merged images (scale bar = 20 μm). R is the colocalization coefficient between green and red fluorescence.

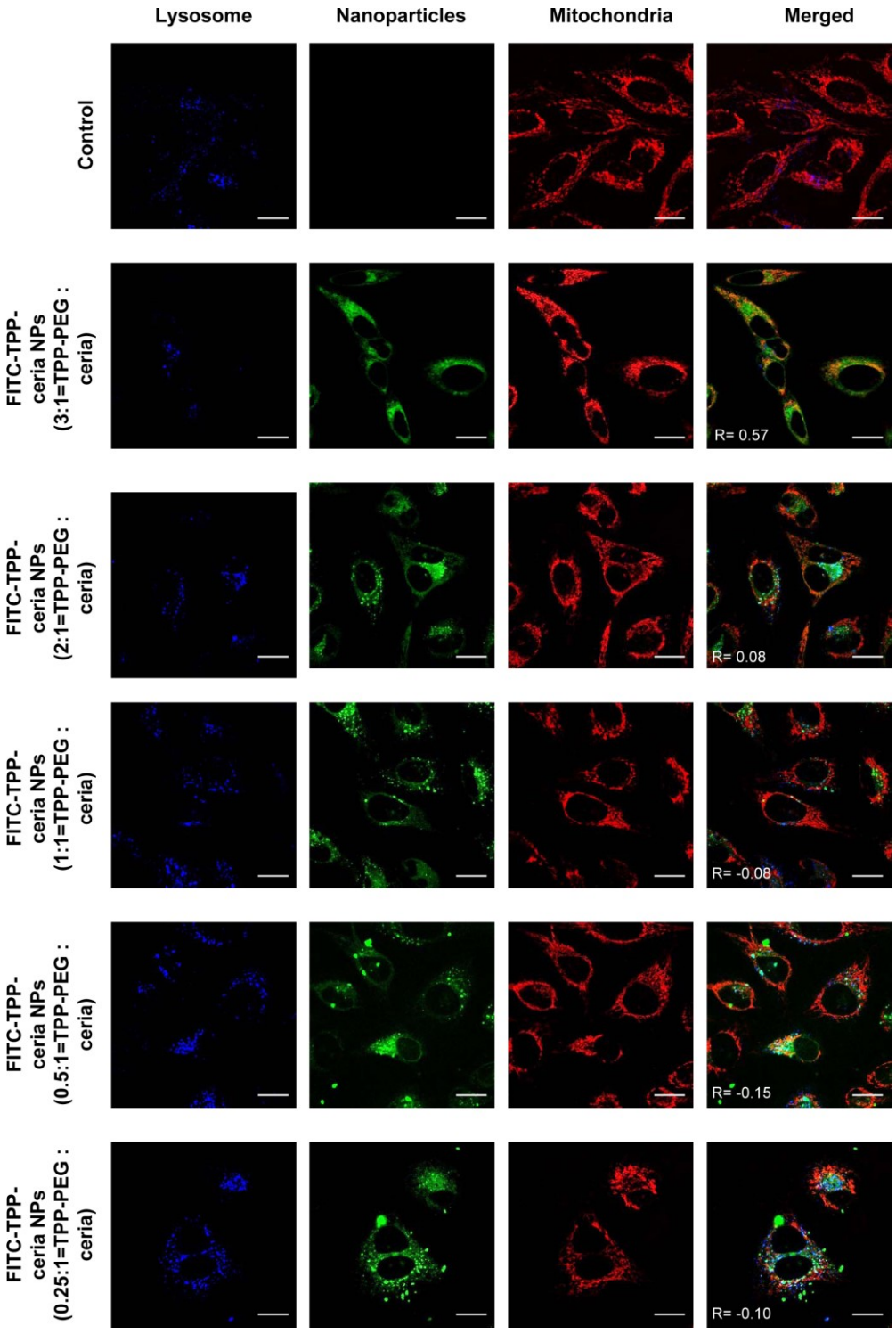

Figure S8. Representative confocal fluorescence microscopy images showing the subcellular colocalization of FITC-conjugated TPP-ceria with different mass ratio of TPP-DSPE-PEG to ceria NPs (green) in HeLa. HeLa cells were stained with LysoTracker (blue) and MitoTracker (red). Colocalization of FITC-conjugated TPP-ceria NPs and mitochondria (red) is shown in merged images (scale bar = 20 μm). R is the colocalization coefficient between green and red fluorescence.

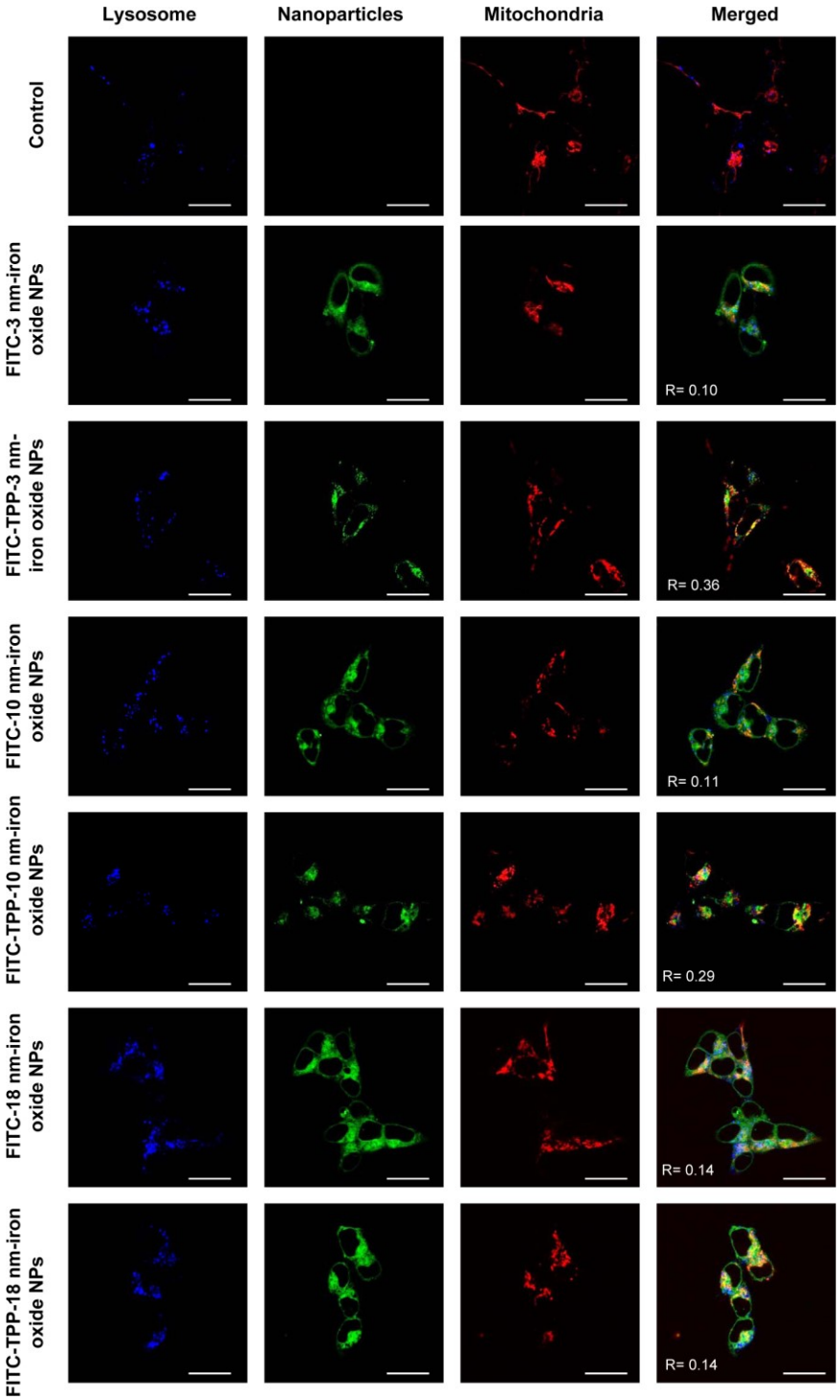

Figure S9. Representative confocal fluorescence microscopy images showing the subcellular colocalization of FITC-conjugated TPP-iron oxide NPs with 3 nm, 10 nm, and 18 nm core size and FITC-conjugated iron oxide NPs with 3 nm, 10 nm, and 18 nm core size in SH-SY5Y. SH-SY5Y cells were stained with LysoTracker (blue) and MitoTracker (red). Colocalization of FITC-conjugated TPP-iron oxide NPs and mitochondria (red) is shown in merged images (scale bar = 20 μm). R is the colocalization coefficient between green and red fluorescence.

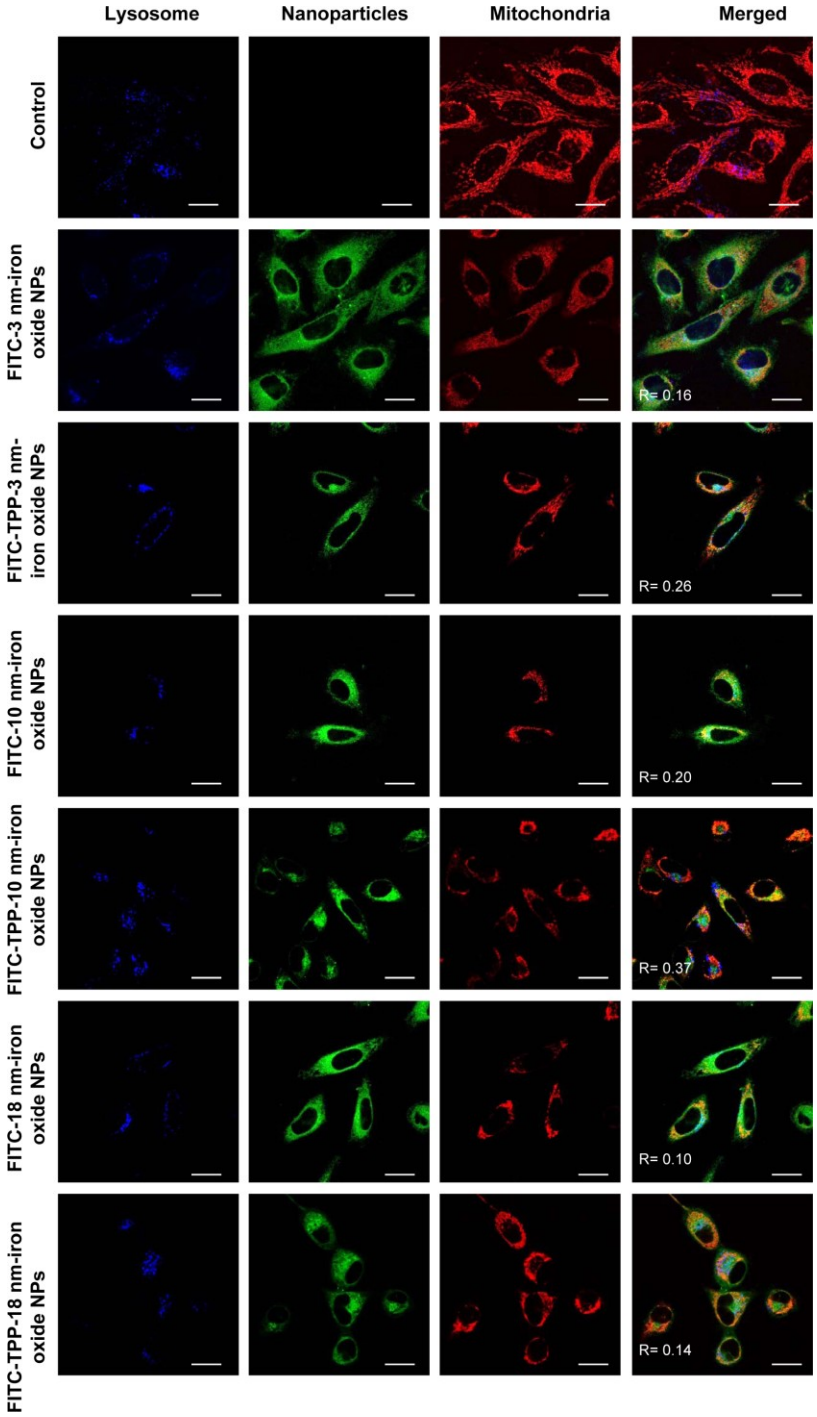

Figure S10. Representative confocal fluorescence microscopy images showing the subcellular colocalization of FITC-conjugated TPP-iron oxide NPs with 3 nm, 10 nm, and 18 nm core size and FITC-conjugated iron oxide NPs with 3 nm, 10 nm, and 18 nm core size in HeLa. HeLa cells were stained with LysoTracker (blue) and MitoTracker (red). Colocalization of FITC-conjugated TPP-iron oxide NPs and mitochondria (red) is shown in merged images (scale bar = 20 μm). R is the colocalization coefficient between green and red fluorescence.

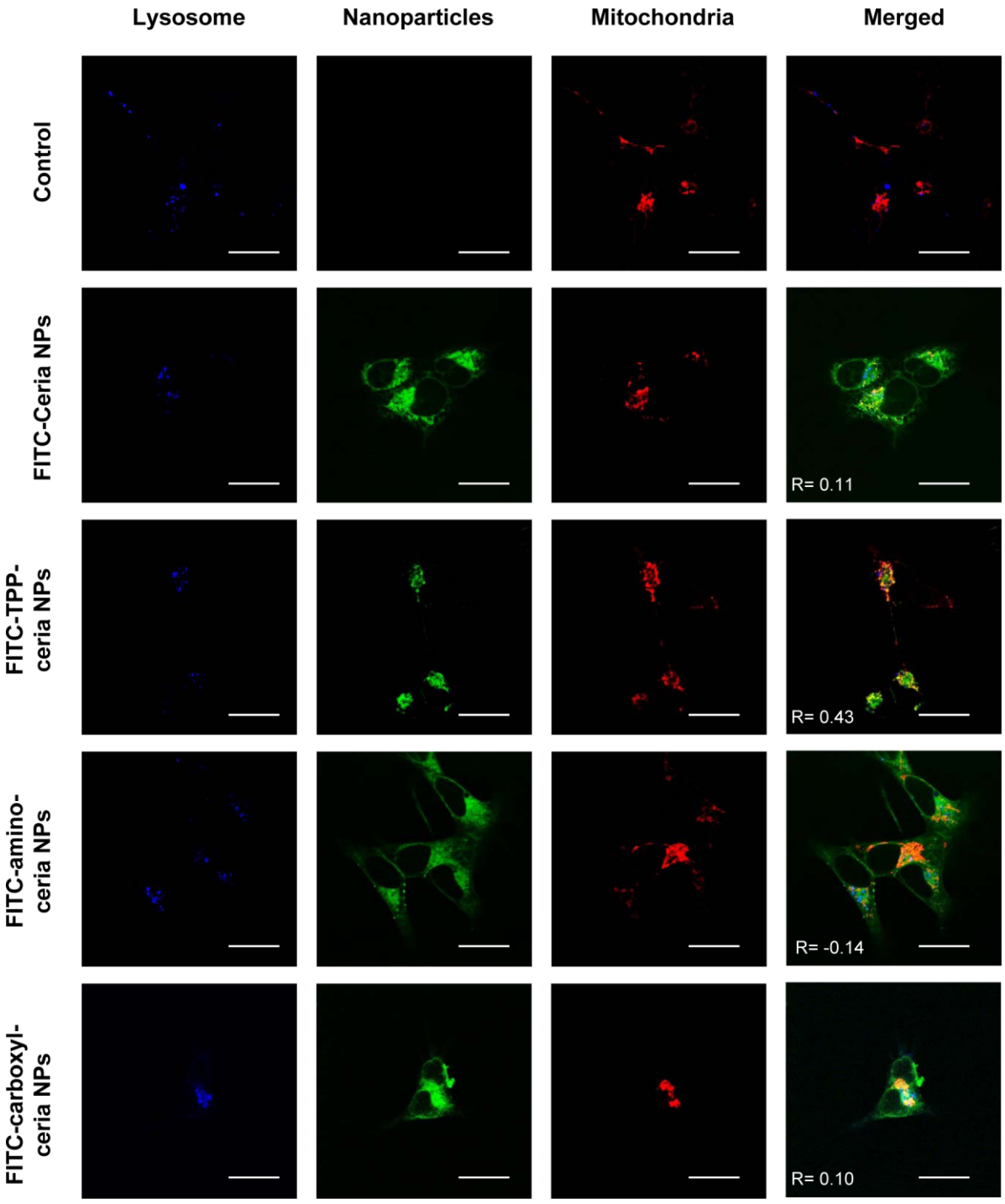

Figure S11. Representative confocal fluorescence microscopy images showing the subcellular colocalization of FITC-conjugated TPP-ceria, FITC-conjugated ceria NPs, FITC-conjugated carboxyl-ceria NPs and FITC-conjugated amino-ceria NPs (green) in SH-SY5Y cells. SH-SY5Y cells were stained with LysoTracker (blue) and MitoTracker (red). Colocalization of FITC-conjugated TPP-ceria NPs and mitochondria (red) is shown in merged images (scale bar = 20 μm). R is the colocalization coefficient between green and red fluorescence.

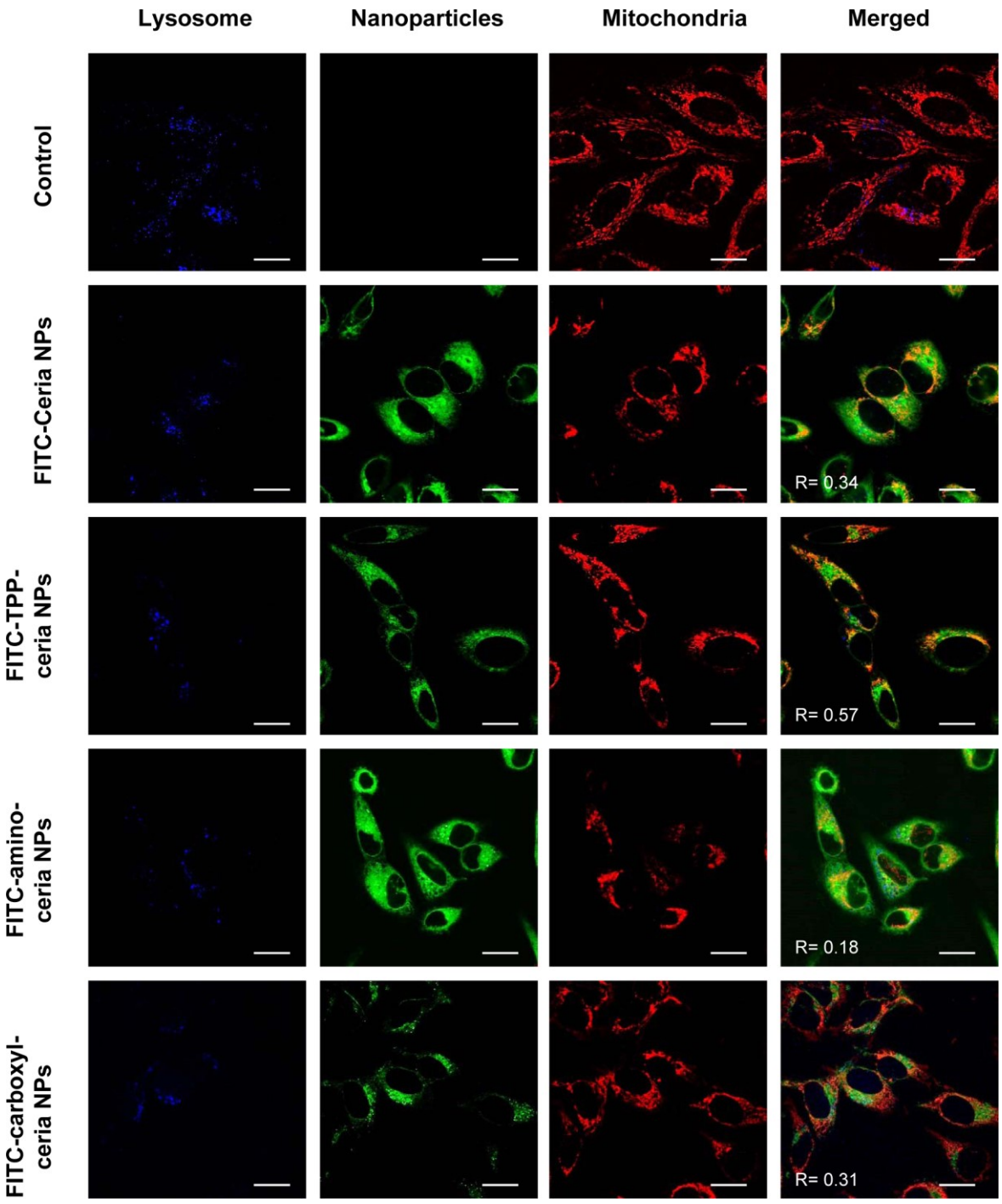

Figure S12. Representative confocal fluorescence microscopy images showing the subcellular colocalization of FITC-conjugated TPP-ceria, FITC-conjugated ceria NPs, FITC-conjugated carboxyl-ceria NPs and FITC-conjugated amino-ceria NPs (green) in HeLa cells. HeLa cells were stained with LysoTracker (blue) and MitoTracker (red). Colocalization of FITC-conjugated TPP-ceria NPs and mitochondria (red) is shown in merged images (scale bar = 20 μm). R is the colocalization coefficient between green and red fluorescence.

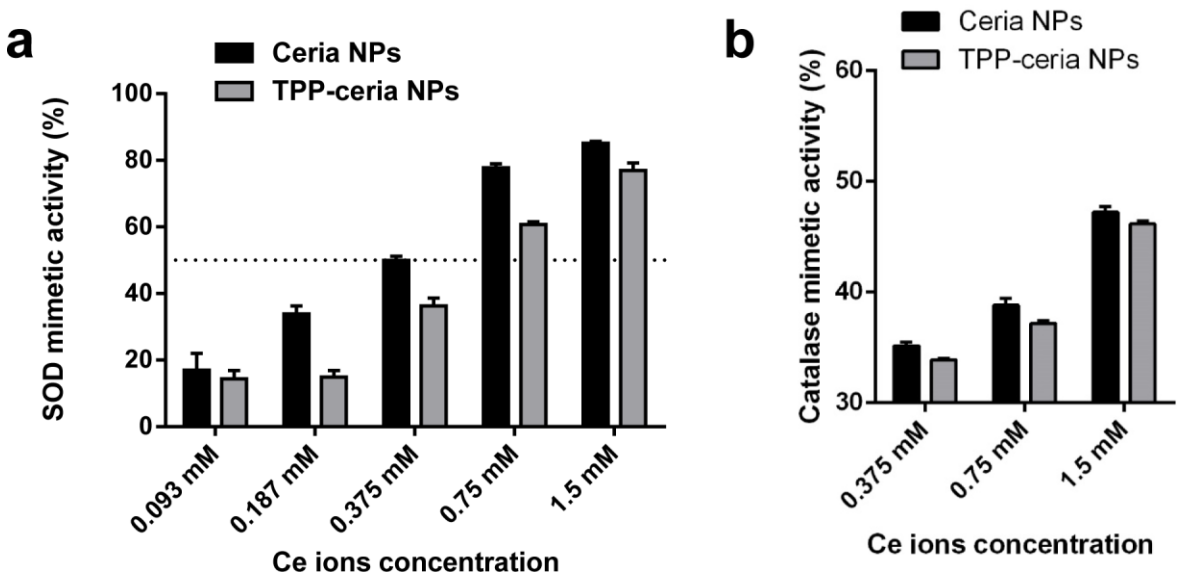

Figure S13. SOD and catalase mimetic activity of ceria NPs and TPP-ceria NPs. a) SOD mimetic activity (n = 9), b) Catalase mimetic activity (n = 9).

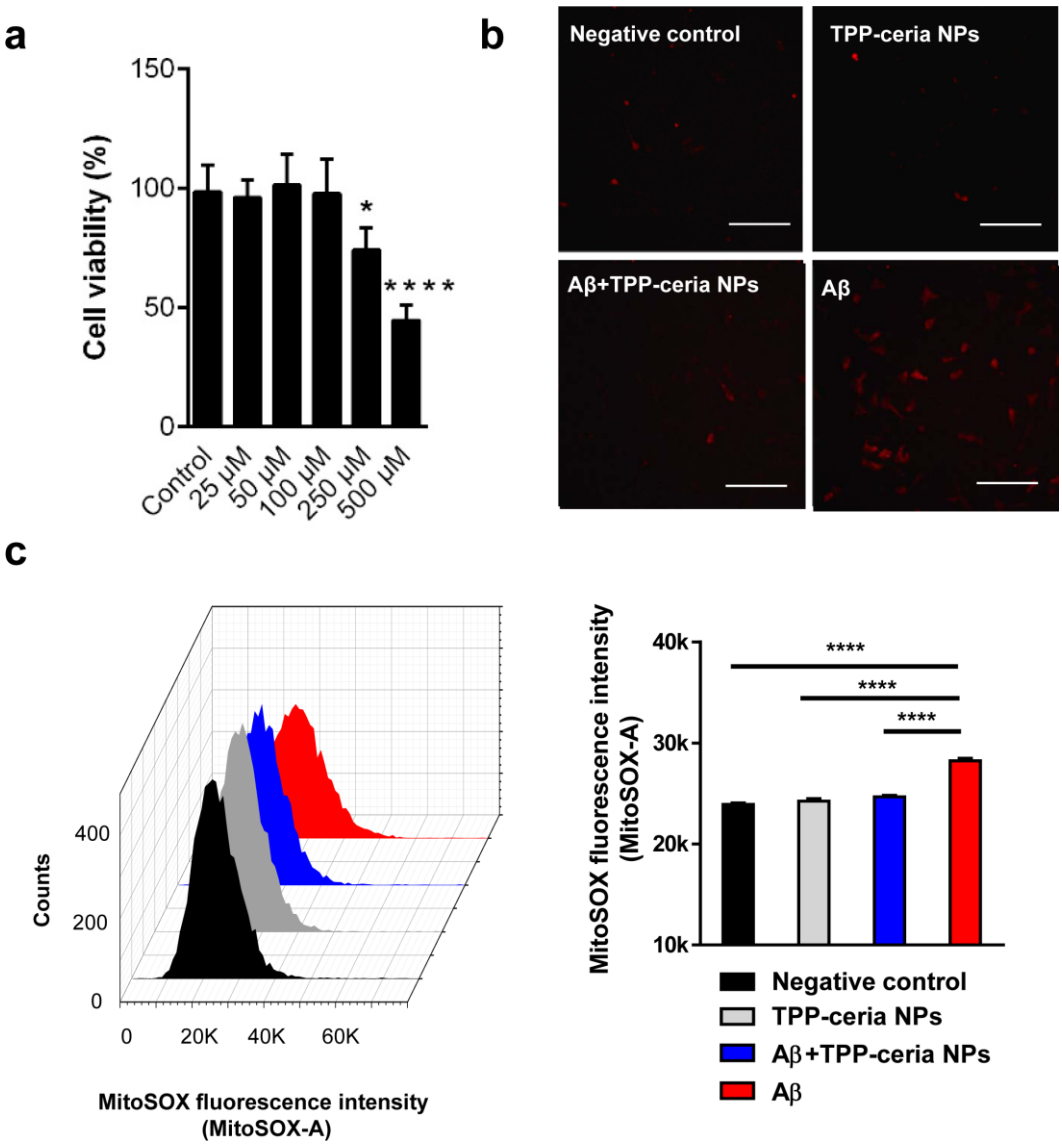

Figure S14. TPP-ceria NPs restore Aβ-induced mitochondrial ROS. a) The toxicity of TPP-ceria NPs were determined by MTT assay. * $p < 0.05$, **** $p < 0.0001$ versus the vehicle treatment. Statistical analysis was performed using an ANOVA test. b) Mitochondrial ROS from HT22 cell line was determined by MitoSOX staining. HT22 cells untreated (negative control), exposed to 0.1 mM TPP-ceria NPs (TPP-ceria NPs), to 5 µM Aβ and 0.1 mM TPP-ceria NPs (Aβ +TPP-ceria NPs), and to 5 µM Aβ (Aβ) for 12 hours were stained using 5 µM MitoSOX. Scale bar = 50 µm. c) Mitochondrial ROS scavenge activity of TPP-ceria NPs in HT22. Fluorescence of MitoSOX® was measured by FACS. Error bars represent a 95% CI.

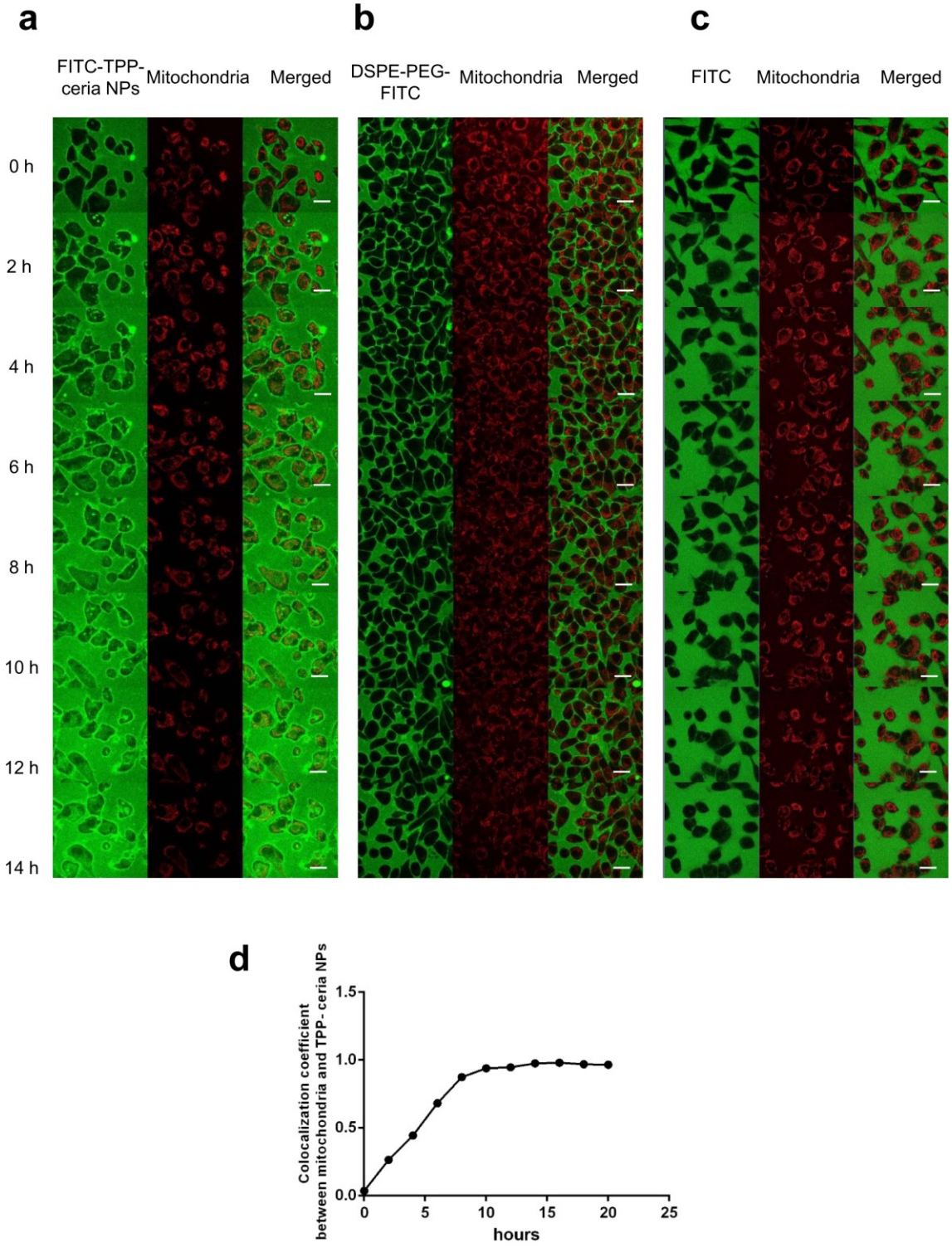

Figure S15. Mechanism of TPP-ceria NPs movement into mitochondria in HeLa cells. Time-serial confocal image of a) FITC conjugated TPP-ceria NPs, b) DSPE-PEG-FITC c) FITC. Scale bar = 20 μm. d) Colocalization coefficient between mitochondria and FITC conjugated TPP‑ceria NPs based on Figure S7A.

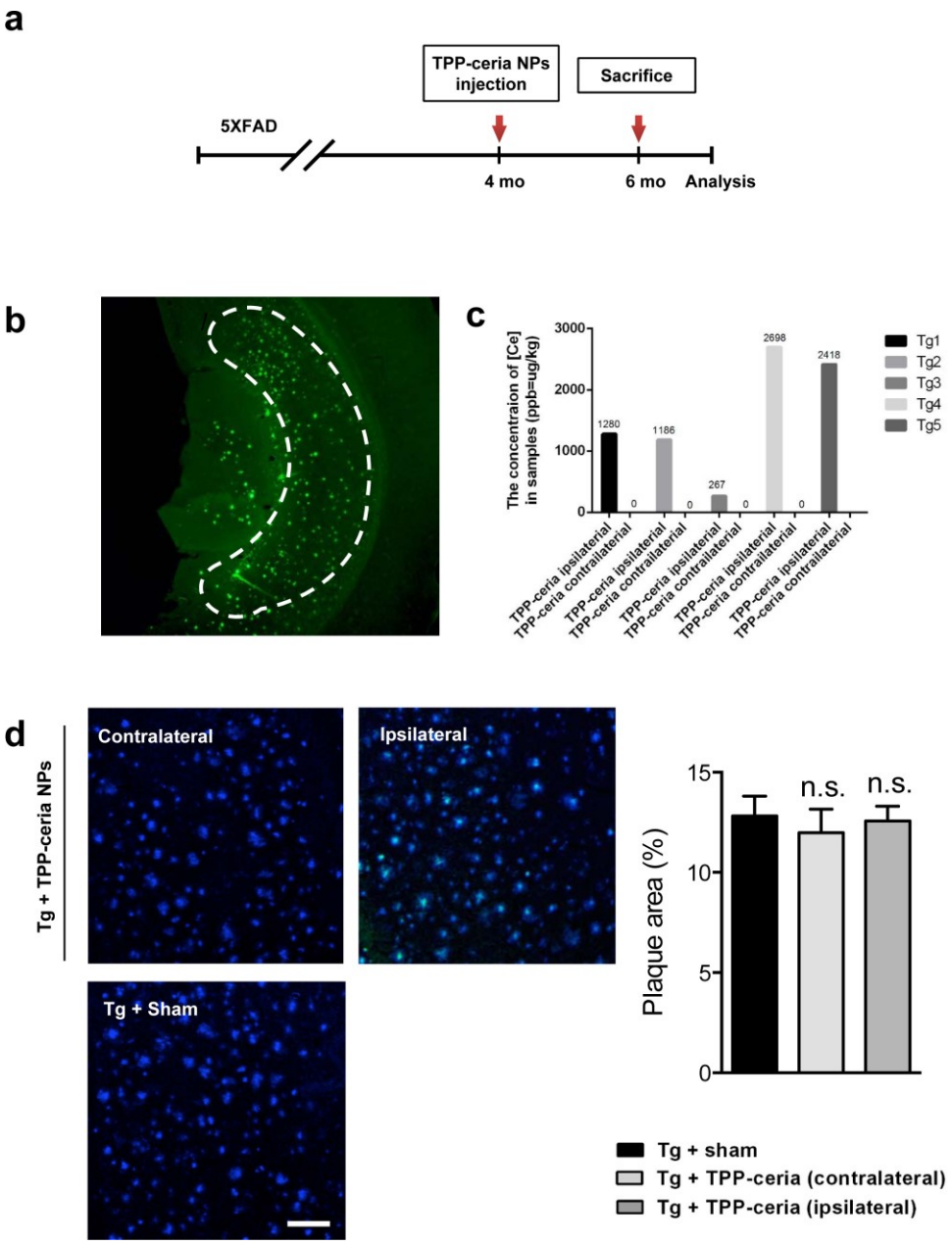

Figure S16. Stereotaxic injection of TPP-ceria nanoparticles into the subiculum of 5XFAD mice. a) Stereotaxic surgery was used to inject FITC-conjugated TPP-ceria NPs or PBS. Mice were sacrificed and the brains analyzed by immunohistochemistry 2 months after injection. b) Confocal microscope image from brain sections of FITC-conjugated TPP-ceria NP-injected mice. c) The concentration of cerium ions in the ipsilateral and contralateral brain tissues were measured by ICS-MS. d) Confocal fluorescence images (left) of Aβ deposition in coronal brain sections stained with FSB (blue). Statistical analysis was performed using an ANOVA test. Scale bar = 50 μm. A plot of plaque area (right). Error bars represent 95% CIs (n = 4 per group).

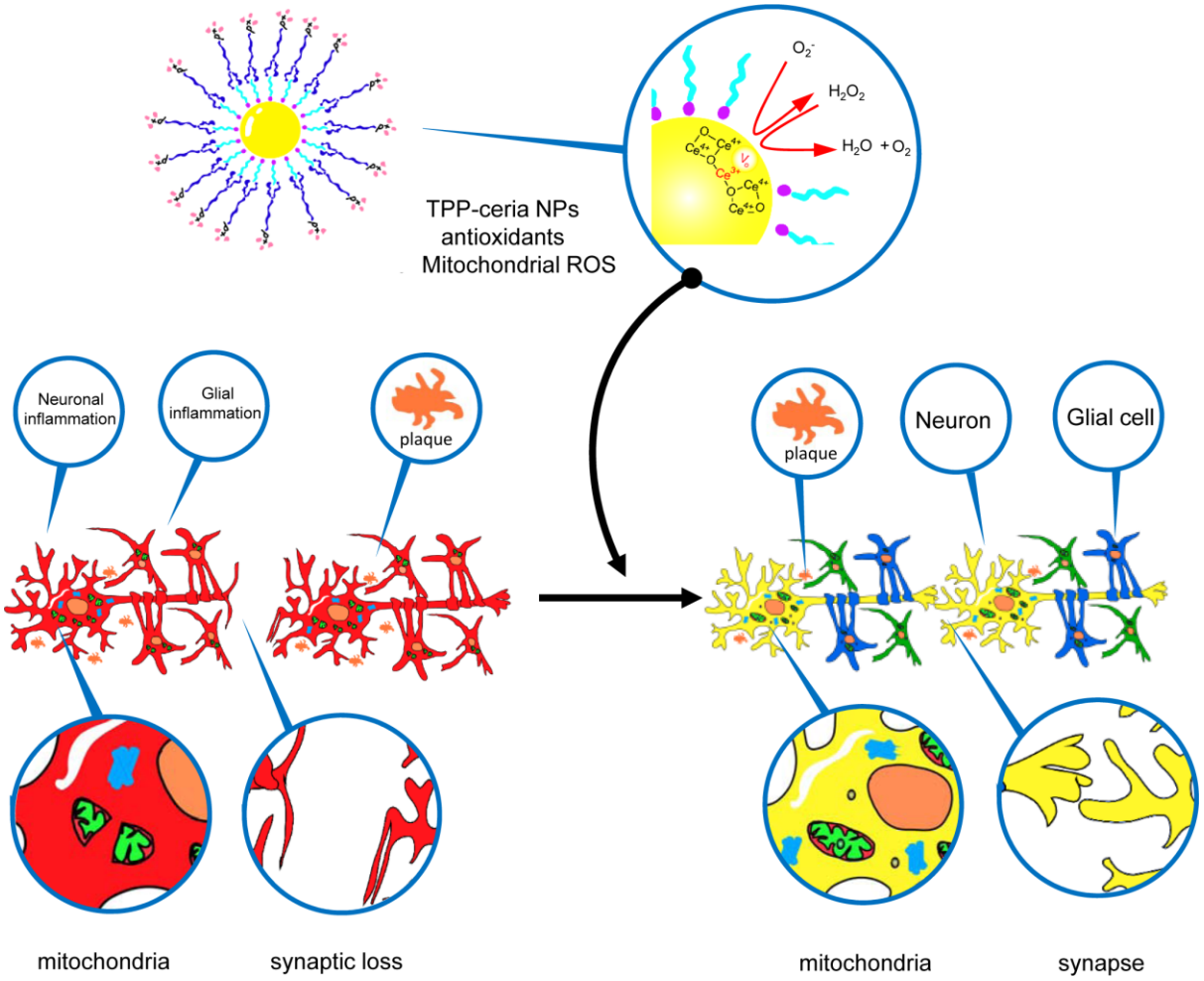

Figure S17. Schematic diagram of therapeutic effects of TPP-ceria NPs. When mitochondria are disrupted by overproduced ROS in AD, cytotoxic inflammation results in injury to adjacent neurons (red). Mitochondria-targeting ceria NPs are subjected to TPP conjugation, rendering their selective uptake into the mitochondrial matrix. Delivered TPP-ceria NPs assist in the maintenance of healthy mitochondrial morphology, synapse formation, and protect neurons by mitigating excessive inflammation (yellow).